Biophysical Chemistry 155 (2011) 74–81

Contents lists available at ScienceDirect

Biophysical Chemistry

journal homepage: http://www.elsevier.com/locate/biophyschem

Molecular mechanism of action for reversible $P2Y_{12}$ antagonists

Haibo Liu [a], Hu Ge [b], Yong Peng [a], Peigen Xiao [a], Jun Xu [b,*]

[a] Institute of Medicinal Plant Development, Peking Union Medical College, Chinese Academy of Medical Sciences, Beijing 100194, PR China
[b] School of Pharmaceutical Sciences, Sun Yat-sen University, 132 East Circle at University City, Guangzhou 510006, PR China

ARTICLE INFO

Article history:
Received 30 January 2011
Received in revised form 2 March 2011
Accepted 2 March 2011
Available online 6 March 2011

Keywords:
$P2Y_{12}$ receptor
ADP
Antagonists
Platelets aggregation

ABSTRACT

Recently, reversible antagonists of the $P2Y_{12}$ receptor have been reported. However, the mechanisms of binding have not been elucidated. To this end, a number of homology models were built by means of three programs from four templates. A consensus model was derived from those initial models. The final model was created by refining the consensus model with molecular dynamics simulations. The agonist and antagonists of $P2Y_{12}$ have been docked in the final model. For the agonist, the Arg256, Lys280, and Phe252 are "hot" residues. For the antagonists, the Lys280 and Phe252 are "hot" residues that have hydrogen bonding contacts and π–π interactions, respectively. These results can explain the observations of mutation experiments and can guide the design of new inhibitors.

1. Introduction

ADP is an important signal molecule for platelet function; it is involved in physiological and pathological responses [1]. Purinergic receptor (P2 receptor) located on the surface of platelet cell membrane is a chemoreceptor for ADP. It can be activated by extracellular nucleotides and triggers the aggregation of platelet [2]. In animal models and in clinical practice, the inhibition of ADP-induced platelet aggregation is an effective approach for treating thrombotic events. Therefore, P2 receptors are the main targets of anti-aggregation agents. The P2 receptor family consists of two classes, the Ca^{2+} channels $P2X_{1-7}$ and G protein-coupled P2Y subtypes. $P2Y_1$ and $P2Y_{12}$ are the most attractive targets among P2Y subtypes for new anti-platelet drugs [3].

In the past decade, there has been an increasing interest on irreversible $P2Y_{12}$ inhibitors [4,5]. Clopidogrel, ticlopidine, and prasugrel have been developed to reduce atherothrombosis for patients with acute coronary syndromes [6–8] (Fig. 1). Most of the irreversible agents are pro-drugs, thus *in vivo* metabolism is required. They can be activated in the liver by cytochrome P450 enzymes (mainly via CYP 2C19) [6,9]. The active metabolite of clopidogrel, Act-Met, acts through the formation of a disulfide bond with the Cys97 within the first extracellular loop of $P2Y_{12}$ receptor [10] (Fig. 1). The irreversible $P2Y_{12}$ inhibitors are widely utilized in clinical practice. In some cases, the agents can be combined with other drugs for better effect. For example, the administration of asipirin with clopidogrel is more effective than the use of aspirin alone [11–15].

Reversible $P2Y_{12}$ receptor antagonists were reported in 2009 [16–18]. These new inhibitors have a faster onset of action than those of irreversible agents because hepatic activation is not required. Moreover, the degree and lasting time of inhibition is more controllable, and thus, the risk of drug–drug interactions is reduced. Adenosine is the scaffold of the earliest reported reversible agents. These agents include ticagrelor (AZD6140) and cangrelor. Both of them are derived from ATP, which is a natural antagonist of $P2Y_{12}$ [5,19]. The antagonists with other scaffolds, such as piperazinyl–glutamate–pyrimidines [20], piperazinyl–glutamate–pyridines [21], and thienopyrimidines [22], were also discovered [23] (Fig. 1).

A set of mutation experiments have been performed to identify the binding modes of ADP and of the reversible antagonists for the $P2Y_{12}$ receptor. The results revealed that transmembrane helix 6 (TM6) hosts domains that interact with the agonist. The Arg256 and His253 of TM6, and the Lys280 of TM7, are "hot" residues for agonist recognition [24]. However, the binding modes of reversible antagonists are unclear.

Structure-based drug discovery approaches have also been used to clarify the binding modes of reversible antagonists. The crystal structure of the human $P2Y_{12}$ receptor is not available at this time. Thus a number of homology models have been built to investigate the interactions between the ligands and the receptor. Most of the models were built from the bovine rhodopsin template [25–27]. The earliest model, built by Costanzi in 2004, seems to be the best[25].

Turkey beta1 adrenergic receptor and squid rhodopsin have been reported in 2008 [28,29]. The two proteins seem to provide better templates for the modeling of $P2Y_{12}$ receptor. In this paper, we have attempted to build a better homology model for the $P2Y_{12}$ receptor. Based upon the new model, the binding modes of the agonist ADP and reversible antagonists are investigated.

* Corresponding author. Tel.: +86 20 3994 3074.
E-mail addresses: wavingsea2008@gmail.com (H. Liu), klmh001@yahoo.com.cn (H. Ge), ypeng@implad.ac.cn (Y. Peng), xiaopg@public.bta.net.cn (P. Xiao), xujun9@mail.sysu.edu.cn (J. Xu).

0301-4622/$ – see front matter © 2011 Elsevier B.V. All rights reserved.
doi:10.1016/j.bpc.2011.03.001

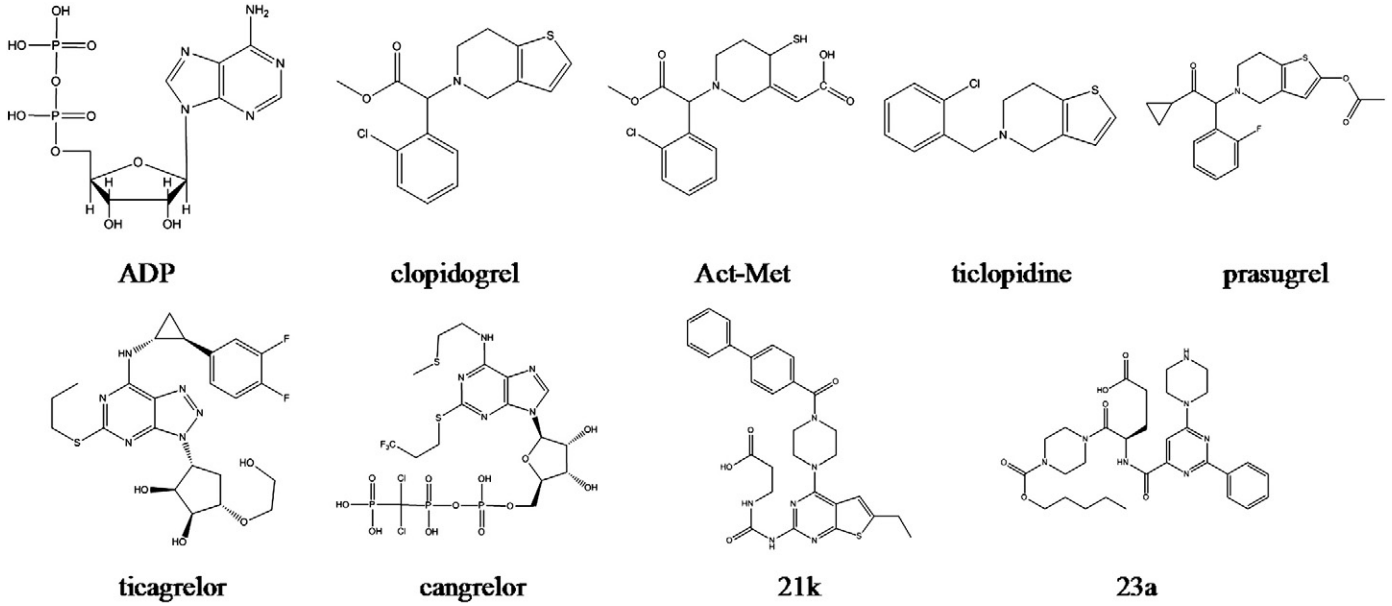

Fig. 1. The agonist (ADP) and antagonists of $P2Y_{12}$ receptor. Clopidogrel, ticlopidine and prasugrel are irreversible antagonists; ticagrelor, cangrelor, 21 k and 23 a are reversible antagonists; Act-Met is the active metabolite of clopidogrel.

2. Methods

The $P2Y_{12}$ receptor belongs to the adenosine class of heterotrimeric guanine nucleotide-binding protein-coupled receptors (GPCRs). GPCR receptors play important roles in drug discovery [30]. Due to the difficulty of crystallizing these receptors, homology modeling is the main approach for GPCR structure-based drug design [31].

2.1. BLAST retrieval

The amino acid sequences of the $P2Y_{12}$ receptor (Swiss-Prot number: Q9H244) were retrieved through a Basic Local Alignment Search Tool (BLAST) [32,33]. This was performed with the BLASTP online program at http://blast.ncbi.nlm.nih.gov/Blast.cgi. The sequences of the Protein Data Bank (PDB) databases were searched. The sequences with higher identities, positive scores, and smaller e-values were selected as candidate templates (Table 1). Three proteins were elected from fifteen protein hits. The Turkey beta1 adrenergic receptor, reported in 2008 [29], was ranked as the most favored homology template.

The alignment errors increase rapidly when the sequence identity of two proteins is less than 30% [34]. The sequence identity is usually less than 25% [31] for GPCR homologues. Therefore, the automated homology modeling of GPCRs is likely to result in more errors [35]. The errors in alignments cannot be justified by energy optimizations, molecular dynamics, or distance geometry refinements. However, the alignments are critical to the quality of the homology model. Thus, multiple-sequence alignments are adopted in order to enhance the alignment quality.

Homology models of the $P2Y_{12}$ receptor were constructed with different combinations of three modeling programs and three protein structure templates (PDB IDs: 2VT4, 1HLL and 2Z73). The programs are the SWISS-MODEL online modeling server [36,37], the MODELLER 9v7 [38–40], and the homology modeling module of the Molecular Operating Environment (MOE) [41].

2.2. Modeling with MOE

M1 and M5 were built by means of the homology module in MOE. MOE performs multiple-sequence alignments in four steps: (1). a tree-based alignment was applied to create initial pair-wises; (2). the initial alignment was refined by a single round-robin series of realignments; (3). randomized iterative refinement was applied to reduce sensitivity to the order in which the chains were processed and (4). structure-based re-alignment was applied to re-align the alpha carbon populated chains.

The homology modeling was accomplished in four steps: (1). partial geometry specification; (2). insertions and deletions; (3). loop selection and side chain packing and (4). final model selection and refinement.

The AMBER99 force field was applied to the homology modeling. The carboxyl-terminal and amino-terminal modeling was disabled. The scoring method was GB/VI[42]. Ten models were built by MOE, kept in a MOE database, and ranked by the GB/VI scores.

Table 1
The BLAST search on the sequence of the $P2Y_{12}$ receptor.

Protein name	PDB ID	Score	Expect	Identities	Positives	Gaps
Turkey beta1 adrenergic receptor	2VT4	53.9 (128)	1e-07	68/275 (24%)	118/275 (42%)	35/275 (12%)
Bovine rhodopsin	1JFP, 1LN6, 1HZX, 1GZM and 1F88	38.9 (89)	0.003	56/278 (20%)	104/278 (37%)	35/278 (12%)
Squid rhodopsin	2Z73	31.6 (70)	0.44	20/82 (24%)	36/82 (43%)	0/82 (0%)

Table 2
Profile of seven homology models.

Models	Modeling engine	Template	Contributions	Outlier spots/ sequence
M1	MOE Homology Model	2VT4-B	TM3	14/296 (4.7%)
M2	MODELLER 9v7	2VT4-B	TM2 and eLP1	11/342 (3.2%)
M3	SWISS-MODEL Repository	1HLL	TM4 and eLP2	7/289 (2.4%)
M4	SWISS-MODEL Workspace	2Z73-A	TM5, cLP3 , TM6, eLP3 and TM7	9/336 (2.7%)
M5	MOE Homology Model	2Z73-A	cLP2	8/342 (2.3%)
M6	MODELLER	1F88-A	TM1 and cLP1	11/302 (3.6%)
M7				2/290 (0.7%)

M6 was built by Costanzi in 2004. Plot number in Ramachandran Plots.

2.3. Modeling with MODELLER

M2 was built in MODELLER 9v7 from the protein structure template, 2VT4A. The 3D model was built by optimizing the molecular Probability Density Functions (PDF). This optimization minimized the number of steric violations. The molecular PDF was derived from the individual spatial features of the molecule.

2.4. Modeling with SWISS-MODEL

M3 and M4 were built by means of the SWISS-MODEL program. M3 was taken from the SWISS-MODEL Repository, which was generated by the automated homology modeling pipeline [43–45]. M4 was built using the automatic modeling mode of the SWISS-MODEL Workspace program [36].

2.5. The consensus model

As shown in Table 2, five models (M1–M5) were constructed with different combinations of three modeling programs and three protein structure templates. M6 is the model built by Costanzi (PDB ID: 1Y9C). The six models, M1–M6, were superimposed in the MOE. The consensus model was built based on consensus building blocks in M1–M6.

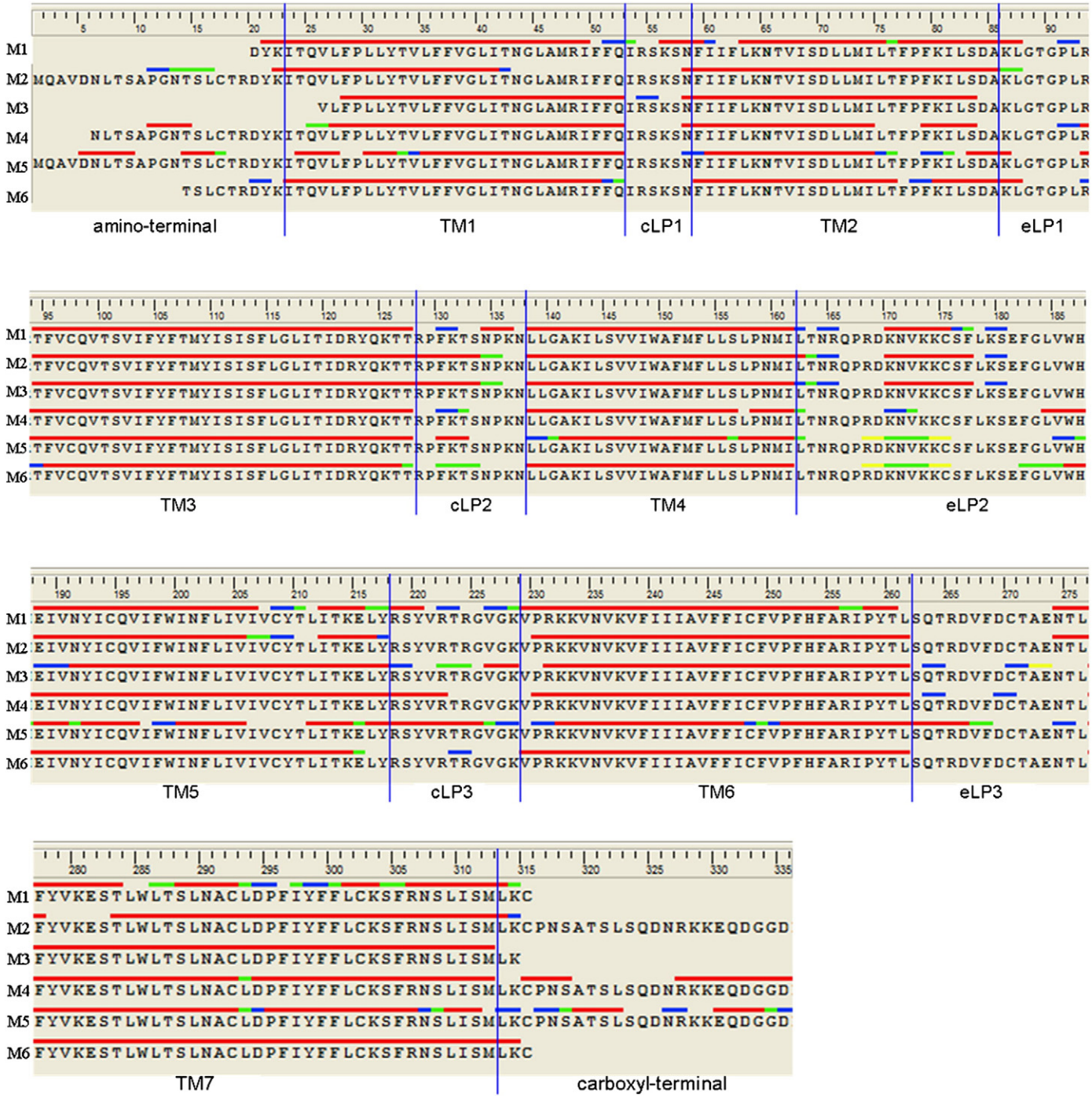

Fig. 2. Alignment of the six homology models for building M7. The secondary structure assignments are annotated with color-coded bars above the sequences. Helixes are in red, strands are in yellow, 1–4 turns are in blue and 1–5 turns are in green. The starting and ending positions of loops in the final model M7 are annotated with blue lines.

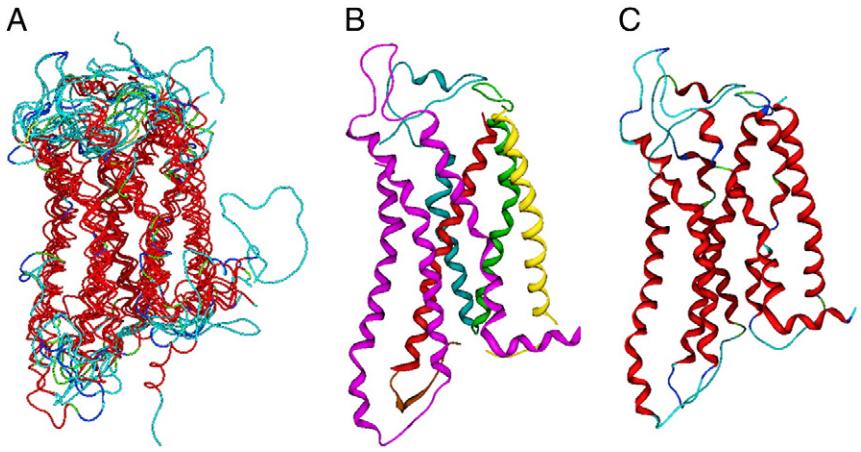

Fig. 3. The conformations of the six models and the resulting conformation of M7. (A) Superimposed template models M1–M6; (B) the building blocks of M7: red (from M1), green (from M2), blue (from M3), purple (from M4), brown (from M5), yellow (from M6) and (C) the final 3 D structure of M7.

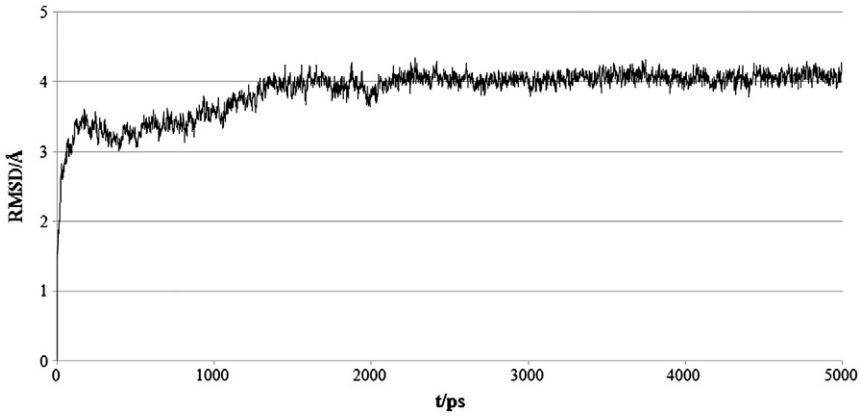

Fig. 4. The RMSD fluctuation of M7 during MD simulation.

The six models, M1–M6, (Table 2) were loaded into the MOE program and aligned. The three-dimensional structures were superimposed. The spatial overlap was maximized. The superposition highlighted conserved regions and diverged regions.

Each model was split into fifteen sections: seven TMs, three extracellular loops (eLP), three cytoplasmic loops (cLP), and the carboxyl-terminal and amino-terminal regions. Since the carboxyl-terminal and amino-terminal regions do not impact the active site pocket, they were truncated. The starting and ending positions of each TM helix were compared throughout all six models. The consensus TM conformations were picked as building blocks for the consensus homology model. The thirteen loops of the consensus model were formed by taking templates from the models M1–M6; these building blocks were then connected and the energy minimized. The resulting model was saved in MOE as M7.

2.6. Molecular dynamics simulations

Partial charges for all atoms in M7 were calculated. Then, the energy of M7 was minimized by means of AMBER99 force field, and the ending

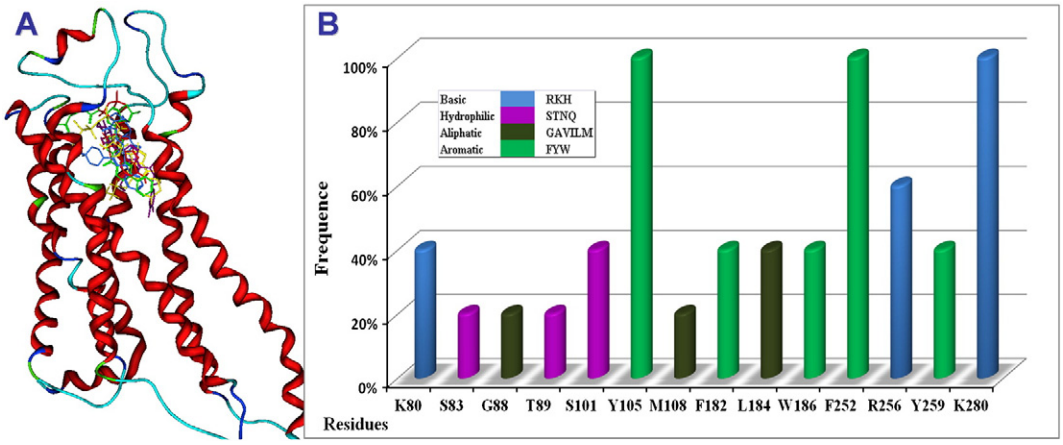

Fig. 5. A: $P2Y_{12}$ homology model with five ligands. B: "Hot" residues derived from the consensus interaction sites with the five ligands.

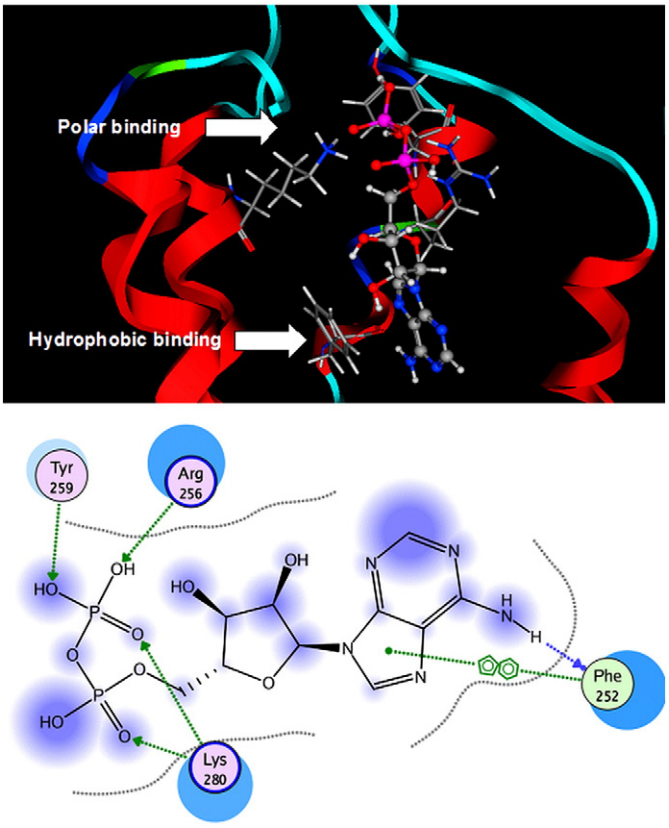

Fig. 6. The ADP binding mode. Top: the pose of ADP in the binding pocket. Bottom: ligand interaction map.

condition of the calculation was the root mean square (RMS) of the two conformer energies being less than 0.1 kcal mol^{-1} $Å^{-1}$. Furthermore, molecular mechanics (MD) simulations were applied in amber 11 [46] on M7. Atoms were allowed to relax by a 2000-step minimization at 300 K with a time step length of 0.002 ps. After the minimization, the atoms in the active site were set flexible for conformation changes. The active site consists of the residues that are 8 Å away from Arg256. The system was gradually heated from 0 K to 300 K in 200 ps. Periodic boundary dynamics simulations of 5 ns were carried out with an NPT (constant composition, pressure, and temperature) ensemble at 1 atm and 300 K. The temperature was kept at 300 K by means of the weak-coupling algorithm. The SHAKE algorithm was used to fix all covalent bonds containing hydrogen atoms with a time step of 2 fs. The Particle-Mesh-Ewald (PME) method was performed to treat long-range electrostatic interactions. A residue-based cutoff of 10 Å was utilized for the non-covalent interactions. The output trajectory files were saved every 2 ps.

2.7. Docking

AutoDock 4.0 [47] was employed for the docking studies. The number of grid points in the x-, y-, and z-axes was set to 60 · 60 · 70, respectively, with grid points separated by the default distance of 0.375 Å. The grid box was centered on the ligand. The hypothetical "hot" residues, Arg256, His253, and Lys280, were set to be flexible. No explicit water molecules were added during docking simulation. Solvation and entropic effects were not taken into account either.

The preferred binding mode was picked, based upon compatibility with the reported mutation results and binding data, as well as energetic considerations, from the ten resulting receptor–ligand complexes. A further refinement was done in MOE. The residues within 10 Å from the ligand were set to be flexible. Energy minimization was carried out by conjugated gradient minimization with the MMFF94x force field. Finally, two types of ligand–receptor interaction diagrams were depicted.

3. Results

The secondary structures of six models (M1–M6) are compared, as shown in Fig. 2. The structures of seven TMs are fairly consistent throughout all six models. The aligned sequences are partitioned into fifteen sections. For each section, the fragment that represents the most common secondary features is picked as a building block for M7 (the resulting homology model). As shown in Fig. 3b and Table 2, M7 is formed from one fragment of M1 (red), two fragments of M2 (green), two fragments of M3 (blue), five fragments of M4 (purple), one fragment of M5 (brown), two fragments of M6 (yellow). M4 contributes the greatest number of the structural building blocks to M7. Three M7 TMs, TM5, TM6, and TM7, are from M4. These TMs are additionally important because these domains contain "hot" residues, such as Arg256 and Lys280.

The RMSD trajectory of MD simulations performed on the M7 was shown in Fig. 4. The system reached equilibrium within 300 ps. The RMSD fluctuating range is 4 Å. The conformations of the M7 model are stabilized after 300 ps. As shown in Fig. 3, the final model (Fig. 3c) is close to the average conformation of the six template models (Fig. 3a).

Ramachandran Plots [48] were generated for the final model (M7) and for the other models (M1–M6). The number of outliers for each model was the criterion that was used to assess the consistency of the models' stereochemistries. Ramachandran dihedral plots for the seven models were shown in a supplementary data sheet. The number of the outliers for each model is listed in Table 2. Fewer outliers indicate a higher quality model. For M1–M6, the number of outliers range from seven to fourteen. M7 has only two outliers in its Ramachandran dihedral plot. More than ninety-nine percent of the coordinates of the residues remained in the appropriate regions (within the green curve areas) of the Ramachandran Plots. The residues that correspond with the two outliers are Arg128 and Phe130. These residues are located in the cLP2 region; this region is irrelevant to the active sites.

Docking experiments were carried out to explore the binding modes of the agonist (ADP) and of the antagonists. Five ligands, one agonist (ADP) and four reversible antagonists, ticagrelor, cangrelor, piperazinyl–glutamate–pyrimidine(23a) [20], and thienopyrimidine-based inhibitor (21k) [23], were built in the MOE Builder. Their three-dimensional structures were energy minimized by MOE using the MMFF94x force field. The initial poses were assigned by the Flexible Alignment module of MOE, which used the ligand from 2VT4.

Table 3
Interaction of the ligands and the $P2Y_{12}$ receptor: the binding free energy and the key residues involved in the interaction.

Ligands	Binding free energy (kcal mol^{-1})			Binding types		
	Total	vdw	ele	Hydrogen bonds (score)	π–π	π–cation
ADP	−129.05	17.67	−146.72	Arg256 (70%), Phe252(49%), Lys280 (94%, 86%) and Tyr259(74%)	Phe252	
Ticagrelor	−79.27	−7.80	−71.47	Lys280 (84%, 11%), Phe252(14.0%) and Tyr105(95.6%)	Phe252	His253
Cangrelor	−157.65	18.94	−176.58	Lys280 (64%, 10%), Trp186 (31%), Leu184 (15%, 35%), Tyr105 (71%), Lys80 (63%, 67%) and Ser101(98%)	Phe252	
21k	−110.52	−12.68	−97.84	Lys80 (71%) and Thr89 (30%)	Phe252and Tyr259	
23a	−137.91	−0.96	−136.14	Lys280 (36%, 38%, 26%) and Ser101 (100%)	Phe252	Arg256

vdw: van der Waals force and ele: electrostatic force.

The five ligands (Red: ADP; Green: 21K; Blue: 23; Yellow: Cangrelor and Purple: Ticagrelor) were docked to the $P2Y_{12}$ homology structure with the AutoDock program. Fig. 5A shows the locations of the five ligands in the $P2Y_{12}$ three-dimensional structure. These ligands are docked in the same putative $P2Y_{12}$ binding pocket. As shown in Fig. 5B, the "hot" residues are identified by summarizing the interactions between the five ligands and $P2Y_{12}$ by means of MOE.

Tyr105, Phe252, Arg256, and Lys280 are "hot" residues; they are the residues that are the most interactive with the ligands. Aromatic/aliphatic and polar basic interactions are the main contributors to binding affinities. As shown in Fig. 6, the polar interactions are located at the opening of the $P2Y_{12}$ binding pocket, and the pocket is close to the solvent. The aromatic/aliphatic interactions are located at the bottom of the pocket. In this area, the ligand tends to form π–π bindings and

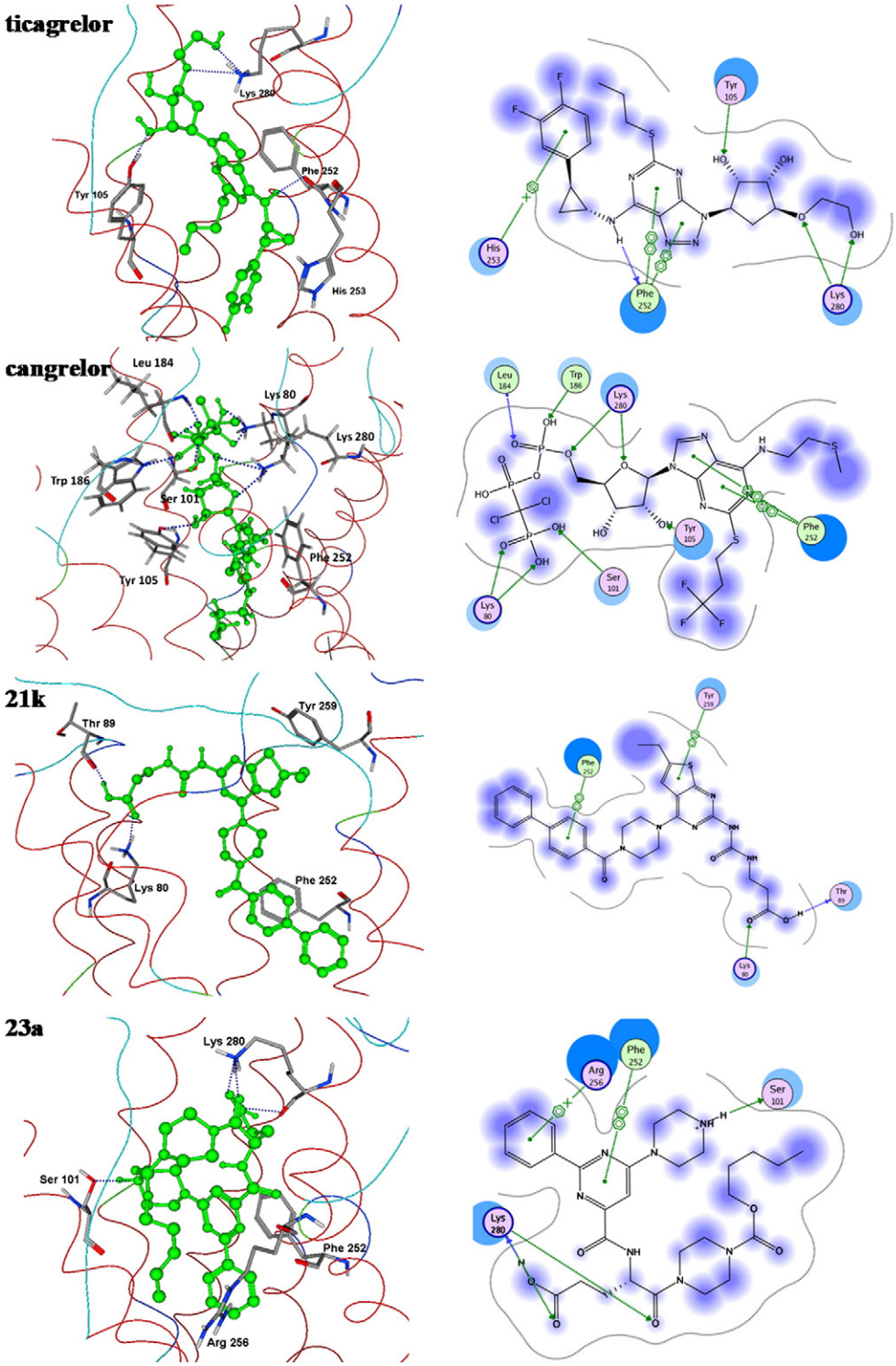

Fig. 7. The binding modes of the four antagonists. Blue arrows represent hydrogen bonds formed with backbone atoms; green arrows represent hydrogen bonds formed with side chain atoms.

hydrophobic interactions with "hot" residues, such as Phe252. Therefore, a good ligand should have polar groups at one end and aromatic/aliphatic groups at the other end.

Fig. 6 shows the interactions between ADP (the agonist) and $P2Y_{12}$. The adenine ring interacts with the bottom of the pocket, and forms a π–π interaction with the Phe252. The polar diphosphate is oriented towards the opening of the pocket, and is partly exposed to the solvent. Three residues in this area (Arg256, Lys280, and Tyr259) form four hydrogen bonds with the phosphate non-bridging oxygen atoms of ADP. All four hydrogen bonds are high-scored as shown in Table 3. Therefore, all three residues are important in these interactions. Additionally, one moderate hydrogen bond was also formed between the Phe252 and the amino-group of ADP.

The four antagonists' binding modes are depicted in Fig. 7. The three-dimensional views are listed on the left and the ligand interaction maps are listed on the right. All the antagonists have the same orientation. The polar ends face the opening of the pocket; here, hydrogen bonds are formed with Lys280, Lys80, Tyr105, and Ser101. The hydrophobic ends point to the bottom of the pocket, and interact, through π–π stacking or π-cation interaction, with Phe252 or His 253, respectively.

Adenine derivatives, ticagrelor and cangrelor, are the antagonists; their binding modes are almost the same. The π–π stacks are formed between Phe252 and the planar adenine rings of the ligands. Lys280 form electrostatic interactions with the oxygen atoms of cangrelor and ticagrelor.

The binding free energies and putative "hot" residues are listed in Table 3. Arg256, Lys280, Tyr105, and Phe252 are the consensus "hot" residues of the binding modes. Electrostatic forces have greater contributions to the four antagonists' binding modes than that of van der Waals forces. Lys280 and Phe252 are the consensus residues that interact with the ligands. The binding affinities of the antagonists are close to that of ADP.

4. Discussion

The binding pocket of $P2Y_{12}$ is surrounded by TM2, TM3, eLP1, eLP2, TM6, and TM7. The pocket is divided into three compartments: I, II, and III (Fig. 8). Compartment I is the entrance of the pocket, and has a number of in hydrogen bonding opportunities. The residues, Lys280 (TM7), Lys80 (TM2), Thr89 (eLP1), Trp186 (eLP2), Leu184 (eLP2), and Tyr259 (TM6), are candidates for interaction with a ligand. Compartment II hosts "hot" residues: Arg256 (TM6) and Ser101 (TM3). Compartment III is hydrophobic and hosts "hot" residues as well: Phe252 (TM6) and His253 (TM6). According to experimental reports [24], compartments II and III are mainly formed within TM6. Costanzi has concluded that Arg256 plays an important role in recognizing ADP. However, A256 does not interact with an antagonist, such as cangrelor [25]. The results (Table 3) of this docking study support Costanzi's observation. As shown in Fig. 8, ADP, ticagrelor, and cangrelor are adenine derivatives. Their binding modes with $P2Y_{12}$ are similar. The adenine scaffold is positioned at compartment III of the binding pocket. For ADP, its adenine scaffold is not substituted by a larger functional group. Consequently, ADP can reach the bottom of the binding pocket. However, the antagonists' adenine scaffold is substituted by two larger hydrophobic groups. Therefore, the antagonists cannot reach the bottom of the pocket. Consequently, Arg256 can form a hydrogen bond with ADP, but cannot form a hydrogen bond with the antagonists. On the other hand, Phe252 forms stronger π–π interactions with the antagonists than with the adenine scaffold. The larger hydrophobic groups create more van de Waals interactions. Cangrelor and 23a have more binding interactions with polar residues, such as, Tyr105, Lys80, and Ser101 (Fig. 8).

Based upon the above analyses, the Phe252 at TM6 is proposed as the "hot" residue of $P2Y_{12}$. Mutation experiments have proved that the His253 is a "hot" residue for recognizing the ligands [24]. This is because His253 is close to Phe252, which forms a π–π interaction with all the ligands.

The binding mode of cangrelor can be changed by the mutation on Ser101 [25]. This hypothesis is supported by the docking result of cangrelor. A stronger hydrogen bond is formed between Ser101 and the terminal phosphate group of cangrelor. Another antagonist, 23a, can also form a strong hydrogen bond between Ser101 and the protonated N atom of 23a. These two examples support the inference that Ser101 plays an important role in the recognition of some antagonists. In contrast, Tyr259 is considered to be a crucial residue for the recognition of ADP. This is also supported by docking results. However, since Tyr259 only interacts with one antagonist, 21K, the residue does not seem as important in the binding of the antagonists.

These findings are helpful for the design of new $P2Y_{12}$ inhibitors. Typical inhibitors mainly have a hydrogen binding moiety and a lipophilic moiety. An aromatic ring in the lipophilic moiety may enhance the binding affinity between the receptor and the ligands.

5. Conclusions

A new $P2Y_{12}$ homology model was built, based on a multi-template consensus approach. This involved the generation of multiple segments within the model from other models or crystal structures, as based on multi-sequence alignments and secondary structure analysis. The model has been validated by agonist and antagonist docking studies. The "hot" residues are identified by

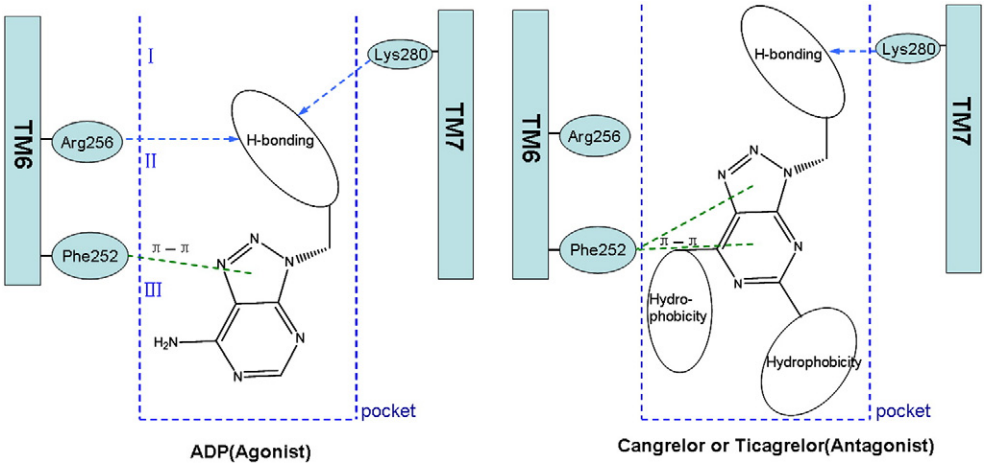

Fig. 8. The three compartments binding modes for ADP and the antagonists. The adenine rings of the antagonists cannot reach the bottom of the pocket due to larger hydrophobic groups.

ligand–receptor consensus studies. The model and docking studies have explained experimental observations (the agonist and the antagonists bind at the same binding pocket in different modes). The former does not reach the bottom of the pocket; however, it forms hydrogen bonds with Lys280 and Arg256, and establishes a π–π interaction with Phe252. The adenine rings of the antagonists cannot reach the bottom of the pocket due to larger hydrophobic groups; they also have strong hydrogen binding interactions with Lys280 and establish stronger π–π interactions with Phe252. However, they lose hydrogen bonds with Arg256. Based on these data, we believe that Lys280, Phe252 and Arg256 are the hot residues.

Acknowledgements

The authors would like to thank Mr. Heming Xu for assistance in preparing the manuscript. This work was funded, in part, by the Major Scientific and Technological Special Project of the Ministry of Science and Technology of China (2010ZX09102-305), the Guangdong Recruitment Program of Creative Research Groups, and the Fundamental Research Funds for the Central Universities (10ykjc01 and 10ykjc20).

Appendix A. Supplementary data

Supplementary data to this article can be found online at doi:10.1016/j.bpc.2011.03.001.

References

[1] N.J. Cusack, S.M.O. Hourani, Platelet P2 receptors: from curiosity to clinical targets, J. Auton. Nerv. Syst. 81 (2000) 37–43.
[2] G. Burnstock, Purinergic nerves, Pharmacol. Rev. 24 (1972) 509–581.
[3] P. Savi, C. Labouret, N. Delesque, F. Guette, J. Lupker, J.M. Herbert, P2Y12, a new platelet ADP receptor, Target Clopidogrel Biochem. Biophys. Res. Commun. 283 (2001) 379–383.
[4] S. Gardell, Ticlopidine and clopidogrel: antithrombotic agents that block ADP-mediated platelet activation, Perspect. Drug Discovery Des. 1 (1994) 521–526.
[5] B. Springthorpe, A. Bailey, P. Barton, T.N. Birkinshaw, R.V. Bonnert, R.C. Brown, D. Chapman, J. Dixon, S.D. Guile, R.G. Humphries, S.F. Hunt, F. Ince, A.H. Ingall, I.P. Kirk, P.D. Leeson, P. Leff, R.J. Lewis, B.P. Martin, D.F. McGinnity, M.P. Mortimore, S.W. Paine, G. Pairaudeau, A. Patel, A.J. Rigby, R.J. Riley, B.J. Teobald, W. Tomlinson, P.J.H. Webborn, P.A. Willis, From ATP to AZD6140: the discovery of an orally active reversible P2Y12 receptor antagonist for the prevention of thrombosis, Bioorg. Med. Chem. Lett. 17 (2007) 6013–6018.
[6] P. Savi, J.M. Herbert, Clopidogrel and ticlopidine: P2Y12 adenosine diphosphate-receptor antagonists for the prevention of atherothrombosis, Semin. Thromb. Hemost. 31 (2005) 174–183.
[7] D.J. Angiolillo, P. Capranzano, Pharmacology of emerging novel platelet inhibitors, Am. Heart J. 156 (2008) 10S–15S.
[8] S.A. Mousa, W.P. Jeske, J. Fareed, Antiplatelet therapy prasugrel: a novel platelet ADP P2Y12 receptor antagonist, Clin Appl Thromb Hemost 16 (2010) 170–176.
[9] D.J. Angiolillo, J.L. Ferreiro, Platelet adenosine diphosphate P2Y12 receptor antagonism: benefits and limitations of current treatment strategies and future directions, Rev. Esp. Cardiol. 63 (2010) 60–76.
[10] P. Savi, J.L. Zachayus, N. Delesque-Touchard, C. Labouret, C. Herve, M.F. Uzabiaga, J.M. Pereillo, J.M. Culouscou, F. Bono, P. Ferrara, J.M. Herbert, The active metabolite of clopidogrel disrupts P2Y12 receptor oligomers and partitions them out of lipid rafts, Proc. Natl Acad. Sci. USA 103 (2006) 11069–11074.
[11] P. Eriksson, Cost-effectiveness of clopidogrel plus aspirin versus aspirin alone, Ann. Intern. Med. 143 (2005) 464, author reply 464–465.
[12] M. Rothberg, Cost-effectiveness of clopidogrel plus aspirin versus aspirin alone, Ann. Intern. Med. 143 (2005) 464, author reply 464–465.
[13] M.D. Schleinitz, P.A. Heidenreich, A cost-effectiveness analysis of combination antiplatelet therapy for high-risk acute coronary syndromes: clopidogrel plus aspirin versus aspirin alone, Ann. Intern. Med. 142 (2005) 251–259.
[14] K.S. Wong, C. Chen, J. Fu, H.M. Chang, N.C. Suwanwela, Y.N. Huang, Z. Han, K.S. Tan, D. Ratanakorn, P. Chollate, Y. Zhao, A. Koh, Q. Hao, H.S. Markus, Clopidogrel plus aspirin versus aspirin alone for reducing embolisation in patients with acute symptomatic cerebral or carotid artery stenosis (CLAIR study): a randomised, open-label, blinded-endpoint trial, Lancet Neurol. (2010).
[15] T.T. Keller, A. Squizzato, S. Middeldorp, Clopidogrel plus aspirin versus aspirin alone for preventing cardiovascular disease, Cochrane Database Syst. Rev. (2007), CD005158.
[16] S.D. Anderson, N.K. Shah, J. Yim, B.J. Epstein, Efficacy and safety of ticagrelor: a reversible P2Y12 receptor antagonist, Ann. Pharmacother. 44 (2010) 524–537.
[17] S. Husted, J.J. van Giezen, Ticagrelor: the first reversibly binding oral P2Y12 receptor antagonist, Cardiovasc. Ther. 27 (2009) 259–274.
[18] J.H. Oestreich, Elinogrel, a reversible P2Y12 receptor antagonist for the treatment of acute coronary syndrome and prevention of secondary thrombotic events, Curr. Opin. Investig. Drugs 11 (2010) 340–348.
[19] N.B. Norgard, Cangrelor: a novel P2Y12 receptor antagonist, Expert Opin. Investig. Drugs 18 (2009) 1219–1230.
[20] J.J. Parlow, M.W. Burney, B.L. Case, T.J. Girard, K.A. Hall, R.R. Hiebsch, R.M. Huff, R.M. Lachance, D.A. Mischke, S.R. Rapp, R.S. Woerndle, M.D. Ennis, Piperazinyl–glutamate–pyrimidines as potent P2Y12 antagonists for inhibition of platelet aggregation, Bioorg. Med. Chem. Lett. 19 (2009) 6148–6156.
[21] J.J. Parlow, M.W. Burney, B.L. Case, T.J. Girard, K.A. Hall, R.R. Hiebsch, R.M. Huff, R.M. Lachance, D.A. Mischke, S.R. Rapp, R.S. Woerndle, M.D. Ennis, Piperazinyl–glutamate–pyridines as potent orally bioavailable P2Y12 antagonists for inhibition of platelet aggregation, Bioorg. Med. Chem. Lett. 19 (2009) 4657–4663.
[22] B. Sirisha, B. Narsaiah, T. Yakaiah, G. Gayatri, G.N. Sastry, M.R. Prasad, A.R. Rao, Synthesis and theoretical studies on energetics of novel N- and O- perfluoroalkyl triazole tagged thienopyrimidines—their potential as adenosine receptor ligands, Eur. J. Med. Chem. 45 (2010) 1739–1745.
[23] S.W. Kortum, R.M. Lachance, B.A. Schweitzer, G. Yalamanchili, H. Rahman, M.D. Ennis, R.M. Huff, R.E. TenBrink, Thienopyrimidine-based P2Y12 platelet aggregation inhibitors, Bioorg. Med. Chem. Lett. 19 (2009) 5919–5923.
[24] K. Hoffmann, U. Sixel, F. Di Pasquale, I. von Kügelgen, Involvement of basic amino acid residues in transmembrane regions 6 and 7 in agonist and antagonist recognition of the human platelet P2Y12-receptor, Biochem. Pharmacol. 76 (2008) 1201–1213.
[25] S. Costanzi, L. Mamedova, Z.G. Gao, K.A. Jacobson, Architecture of P2Y nucleotide receptors: structural comparison based on sequence analysis, mutagenesis, and homology modeling, J. Med. Chem. 47 (2004) 5393–5404.
[26] C. Zhan, J. Yang, X.C. Dong, Y.L. Wang, Molecular modeling of purinergic receptor P2Y12 and interaction with its antagonists, J. Mol. Graph. Model. 26 (2007) 20–31.
[27] K.A. Jacobson, L. Mamedova, B.V. Joshi, P. Besada, S. Costanzi, Molecular recognition at adenine nucleotide (P2) receptors in platelets, Semin. Thromb. Hemost. 31 (2005) 205–216.
[28] M. Murakami, T. Kouyama, Crystal structure of squid rhodopsin, Nature 453 (2008) 363–367.
[29] T. Warne, M.J. Serrano-Vega, J.G. Baker, R. Moukhametzianov, P.C. Edwards, R. Henderson, A.G. Leslie, C.G. Tate, G.F. Schertler, Structure of a beta1-adrenergic G-protein-coupled receptor, Nature 454 (2008) 486–491.
[30] J. Saunders, G-protein-coupled receptors in drug discovery, Bioorg. Med. Chem. Lett. 15 (2005) 3653.
[31] R. Heilker, M. Wolff, C.S. Tautermann, M. Bieler, G-protein-coupled receptor-focused drug discovery using a target class platform approach, Drug Discov. Today 14 (2009) 231–240.
[32] S. Karlin, S.F. Altschul, Methods for assessing the statistical significance of molecular sequence features by using general scoring schemes, Proc. Natl Acad. Sci. USA 87 (1990) 2264–2268.
[33] S.F. Altschul, T.L. Madden, A.A. Schaffer, J. Zhang, Z. Zhang, W. Miller, D.J. Lipman, Gapped BLAST and PSI-BLAST: a new generation of protein database search programs, Nucleic Acids Res. 25 (1997) 3389–3402.
[34] D. Baker, A. Sali, Protein structure prediction and structural genomics, Science 294 (2001) 93–96.
[35] I.D. Pogozheva, M.J. Przydzial, H.I. Mosberg, Homology modeling of opioid receptor–ligand complexes using experimental constraints, AAPS J. 7 (2005) E434–E448.
[36] K. Arnold, L. Bordoli, J. Kopp, T. Schwede, The SWISS-MODEL workspace: a web-based environment for protein structure homology modelling, Bioinformatics 22 (2006) 195–201.
[37] T. Schwede, J. Kopp, N. Guex, M.C. Peitsch, SWISS-MODEL: an automated protein homology-modeling server, Nucleic Acids Res. 31 (2003) 3381–3385.
[38] A. Sali, T.L. Blundell, Comparative protein modelling by satisfaction of spatial restraints, J. Mol. Biol. 234 (1993) 779–815.
[39] A. Fiser, A. Sali, Modeller: generation and refinement of homology-based protein structure models, Meth. Enzymol. 374 (2003) 461–491.
[40] A. Sali, Comparative protein modeling by satisfaction of spatial restraints, Mol. Med. Today 1 (1995) 270–277.
[41] Molecular operating environment, Chemical Computing Group Inc., Sherbrooke Street West, Suite 910, Montreal, H3A 2R7, Canada, 2007, 2007.
[42] P. Labute, The generalized Born/volume integral implicit solvent model: estimation of the free energy of hydration using London dispersion instead of atomic surface area, J. Comput. Chem. 29 (2008) 1693–1698.
[43] F. Kiefer, K. Arnold, M. Kunzli, L. Bordoli, T. Schwede, The SWISS-MODEL Repository and associated resources, Nucleic Acids Res. 37 (2009) D387–D392.
[44] J. Kopp, T. Schwede, The SWISS-MODEL Repository: new features and functionalities, Nucleic Acids Res. 34 (2006) D315–D318.
[45] J. Kopp, T. Schwede, The SWISS-MODEL Repository of annotated three-dimensional protein structure homology models, Nucleic Acids Res. 32 (2004) D230–D234.
[46] D.A. Case, T.E. Cheatham 3rd, T. Darden, H. Gohlke, R. Luo, K.M. Merz Jr., A. Onufriev, C. Simmerling, B. Wang, R.J. Woods, The Amber biomolecular simulation programs, J. Comput. Chem. 26 (2005) 1668–1688.
[47] R. Huey, G.M. Morris, A.J. Olson, D.S. Goodsell, A semiempirical free energy force field with charge-based desolvation, J. Comput. Chem. 28 (2007) 1145–1152.
[48] B.K. Ho, R. Brasseur, The Ramachandran plots of glycine and pre-proline, BMC Struct. Biol. 5 (2005) 1–11.